DOI: 10.1002/chem.200902996

Ligand Association/Dissociation Paths and Ill-Defined Coordination Numbers

Antonio Ruiz-Martínez,[a] David Casanova,[b] and Santiago Alvarez*[a]

Abstract: The continuous shape measures approach provides a means for handling the common situation in which a metal atom presents an ill-defined coordination number. Those cases are characterized by the presence of secondary interactions to Lewis bases at distances significantly longer than those expected for a chemical bond. Systematic ways of analyzing ligand association/dissociation pathways that describe such structures and their application to a variety of specific cases are presented. The concepts and methodology presented here apply to molecules and extended solids as well and provide, when needed, a more flexible and precise stereochemical description of the metal coordination sphere than that of an integer coordination number and the associated polyhedral shape.

Keywords: coordination compounds · Jahn–Teller distortion · ligand association · shape measures · transition metals

Introduction

The description of the coordination sphere around a given atom in a molecular or solid-state structure by a regular polyhedron has been a stereotype in chemistry since the introduction of the tetrahedron by Van'Hoff and Le Bel for organic compounds and of the octahedron by Werner for transition-metal compounds. Recently, Avnir and co-workers and ourselves have devoted some efforts to the description of the coordination spheres of transition-metal atoms from the point of view of their *continuous shape measures*.[1] Within that framework, one describes in a quantitative way how close or how far a set of atoms is from a given ideal shape (e.g., a polyhedron). One of the advantages of such an approach is that one can in many instances accurately describe structures that are along the interconversion path of two polyhedra with the same number of vertices.[2]

A difficult problem is that of the structures with an ambiguous coordination number. In most cases they result from the presence of one or more incipient bonds, as if they were snapshots along a ligand association (or dissociation) pathway. In such pathways, the spectator ligands L do not appreciably change their bonding to the metal atom, whereas weakly bonded ligands X can be considered as entering/leaving groups in the association/dissociation reaction, in which **D** and **A** are the coordination polyhedra of the dissociated complex with coordination number n and of the associated complex with coordination number $n+m$, respectively [Eq. (1)].

$$ML_n\ (\mathbf{D})\ +\ mX \rightleftharpoons MX_mL_n\ (\mathbf{A}) \qquad (1)$$

Three things happen during an association process: 1) the M···X distances decrease, 2) the L-M-L bond angles change to make room for the entering ligand, and 3) the M–L bond lengths slightly increase as the coordination number increases.

A wealth of examples of metal complexes with extra contacts to ligands can be found in the literature. These are termed in a variety of ways that reflect the existence of two degrees of metal–ligand bonding interactions concealed by the simple concept of a coordination number. It is common, for instance, to refer to the Jahn–Teller distorted coordination sphere of Cu^{II} complexes as a 4+2 coordination, for

[a] A. Ruiz-Martínez, Prof. Dr. S. Alvarez
Departament de Química Inorgànica and
Institut de Química Teòrica i Computacional (IQTC-UB)
Universitat de Barcelona
Martí i Franquès 1–11, 08028 Barcelona (Spain)
E-mail: santiago@qi.ub.es

[b] D. Casanova
Institut de Química Teòrica i Computacional (IQTC-UB)
Universitat de Barcelona
Martí i Franquès 1–11, 08028 Barcelona (Spain)

Supporting information for this article is available on the WWW under http://dx.doi.org/10.1002/chem.200902996.

which Pauling proposed the use of a fractional bond order. A fractional bond order (calculated as $n = \exp[(d_1 - d_n)/0.60]$, in which d_1 is the single-bond length) can be as small as 0.1 for copper(II) chlorides.[3] It is also not unusual to find reports of "secondary coordination," a term introduced in the chemical literature by Kretsinger and Cotton in 1963[4] to refer to a weak intermolecular interaction seen in a crystal structure between formally noncoordinated carboxylato groups and a tetracoordinate Zn^{II} ion. This term, however, was only sparingly employed in subsequent decades. It must be noted that in some instances that same expression is used to refer to hydrogen-bonding interactions that do not directly involve the metal center,[5] to a vacant coordination site,[6] or to the second coordination sphere of a metal.[7] The same term has even been used to refer to well-defined bonds between two axial ligands and a square planar Ni^{II} unit, given that they may exist independently.[8] Quite often what the authors mean by secondary coordination is not explicitly stated. For the sake of the present discussion, it is important to stress that "secondary coordination" will be used to describe short contacts (or weak bonds) between a Lewis base and a metal atom.[9] The appreciation of the role that such secondary interactions may have led a group of researchers to say that a family of dithiolene copper complexes is "*blessed* with secondary coordination ability."[8]

Other ways of referring to imprecise coordination numbers in transition-metal chemistry include the naming of some copper(I) complexes as "quasi-two-coordinate" to allude to the weak bonding of additional ligands,[10] or the use of the expression "semi-coordinating interaction,"[11] not to mention the widely recognized "agostic interactions" or secondary coordination of ancillary groups[12] that may help, for example, stabilize low coordination numbers[13] or less common coordination geometries, such as a T-shaped tricoordination[14] or a seesaw tetracoordination.[15]

Among the variety of examples that can be found in the literature, we choose to mention in more detail here only some illustrative ones. A classic case from the field of main group chemistry corresponds to the description of the S_N2 nucleophilic substitution reactions at Cd, Sn, Si, Ge, and B centers,[16] described by way of the structural analysis of compounds with coordination numbers between four and five (Scheme 1). In that study, the reaction pathway was

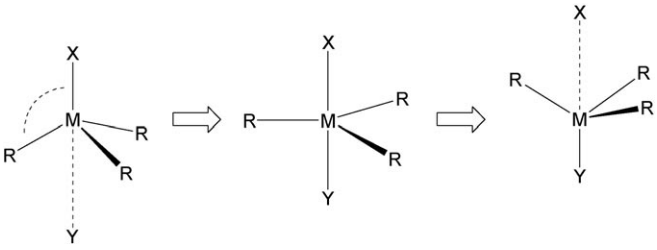

Scheme 1.

calibrated through the M–X and M–Y distances, as well as through the average X-M-R bond angle. In those studies, each molecular structure was considered a snapshot of the dynamic process that goes from reactants to products. This approach is similar to the technique applied by Eadweard Muybridge (1830–1904) in his famous photographic sequence *The Horse in Motion*, with which he resolved the galloping question (i.e., whether at some point during the gallop a horse has all its four hooves off the ground simultaneously).

The complexes of d^{10} metal ions are known to appear as di-, tri-, or tetracoordinate, and structures intermediate between two coordination numbers are often found,[17] referred to, for example, as "quasi-two-coordinate" complexes.[10] In a recent review on *hypocoordinated* multidentate amines,[18] several structures were shown in which one or more nitrogen atoms are not fully coordinated but kept at a relatively short distance from the central metal ion. Hypocoordination of multidentate ligands has also been shown to be important in some spin-crossover systems because a change in coordination number is associated with the change in spin state with temperature.[19,20]

To exemplify how the comparison of structural data for related compounds can provide still images of ligand association/dissociation processes, let us focus on a prototypical solid-state compound, TiO_2 in its anatase polymorphic form. In that structure,[21] the coordination sphere of the Ti ions is significantly distorted from the perfect octahedron (Figure 1, center). A closer look tells us that two of the Ti–O bond lengths are slightly longer than the other four. Even

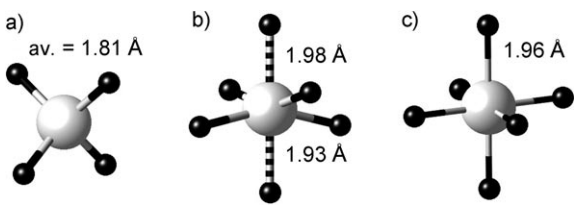

Figure 1. Coordination spheres of a Ti atom in Ba_2TiO_4, anatase, and rutile (from left to right).

Abstract in Catalan: *El mètode de les mesures contínues de forma ens permet tractar la situació trobada freqüentment, en què un àtom metàl·lic presenta un nombre de coordinació no ben definit, caracteritzat per la presència d'interaccions secundàries amb bases de Lewis a distàncies significativament més llargues que les que correspondrien a un enllaç químic. Aquí es presenten formes sistemàtiques d'analitzar els camins d'associació/dissociació de lligands que descriuen aquestes estructures, així com llur aplicació a diverses famílies de compostos. Els conceptes i la metodologia presentats en aquest article s'apliquen tant a molècules com a sòlids infinits i ens proporcionen una descripció estereoquímica més flexible i alhora precisa de les esferes de coordinació que no pas un nombre de coordinació enter i la forma polièdrica associada.*

if the differences in bond lengths are not large, they are associated with a significant deviation of the four equivalent O atoms from the equatorial plane of the ideal octahedron, thus clearly suggesting that the geometry is intermediate between the tetrahedral coordination of Ti in titanates, such as[22] Ba_2TiO_4 or Na_4TiO_4,[23] and the octahedral structure in rutile (Figure 1). By comparing the bond lengths in anatase with those in the titanate, it is clear that the coordination number is larger in the former case. However, comparison of bond lengths in anatase and rutile does not tell us what the *trans* bond angles (155° in anatase, 180° in rutile) reveal: that the Ti atom in the former is en route from the tetrahedron to the octahedron through association of two oxo ions in *trans* positions. Both the bond lengths and angles clearly indicate that anatase is much closer to the octahedron than to the tetrahedron, but each bonding parameter individually would give us a different quantitative estimate of how far we are from the octahedron (or from the tetrahedron). Even Pauling's fractional bond order would be as high as 0.92, thus indicating a much lesser degree of dissociation than the bond angles suggest.

Herein we explore the applicability of continuous shape and symmetry measures to the analysis of coordination geometries that fall along ligand association/dissociation paths. Although we focus here on experimental structural data, the same methodology can be applied to the study of the corresponding reaction pathways in computational studies.[24] The study presented here is by no means comprehensive, yet we discuss a wide variety of examples that showcase the different possible approaches and several paths not reported earlier. We suggest to the reader to choose one of two examples of his/her interest to get a feeling of the possibilities of the approach presented here, and then proceed to the Conclusion. Each case can be then examined later independently when needed.

Results and Discussion

Conceptual and methodological approaches: In the present work, the stereochemistry of the coordination sphere of a metal will be characterized by continuous shape measures[25] and derived parameters.[1] In essence, a continuous shape measure calibrates the deviation of a given structure from an ideal shape,[1,26] such as the octahedron. The octahedral shape measure of a coordination polyhedron, S(OC-6), will be zero if it is perfectly octahedral, and adopt progressively higher positive values as the structure deviates from the ideal. In general, within the present study, we will use systematically the shape measures $S(\mathbf{D})$ and $S(\mathbf{A})$, relative to the fully dissociated and fully associated polyhedra in each particular case analyzed.

Since some of the structures to be studied here present intermediate geometries between the dissociated and the associated polyhedra, it will be useful also to describe each molecule by its position relative to the minimal distortion interconversion path between them by means of two parameters. On one hand, the path-deviation function, $\Delta_{\mathbf{D,A}}(\mathbf{Q})$, measures the distance of a structure **Q** to the minimal distortion pathway (in percentage of the path length) for the **D**↔**A** interconversion.[2] On the other hand, for structures **Q** that are along the minimal distortion path, we can measure the percentage of conversion from one ideal polyhedron to the other one, by means of the generalized interconversion coordinate, $\varphi_{\mathbf{D}\rightarrow\mathbf{A}}(\mathbf{Q})$.[27]

For the systems to be studied, found somewhere along the path of a bond-forming reaction [Eq. (1)], we can distinguish four general cases that can be tackled with different methodological approaches:

*Method **I**: The common fragment ML_n changes its shape from starting to end products, characterized by ideal geometries **D** and **A**, respectively*: This is the case for the TiO_4 group in Figure 1, which goes all the way from the tetrahedron to the square, as sketched in Figure 2, **I**. In such cases,

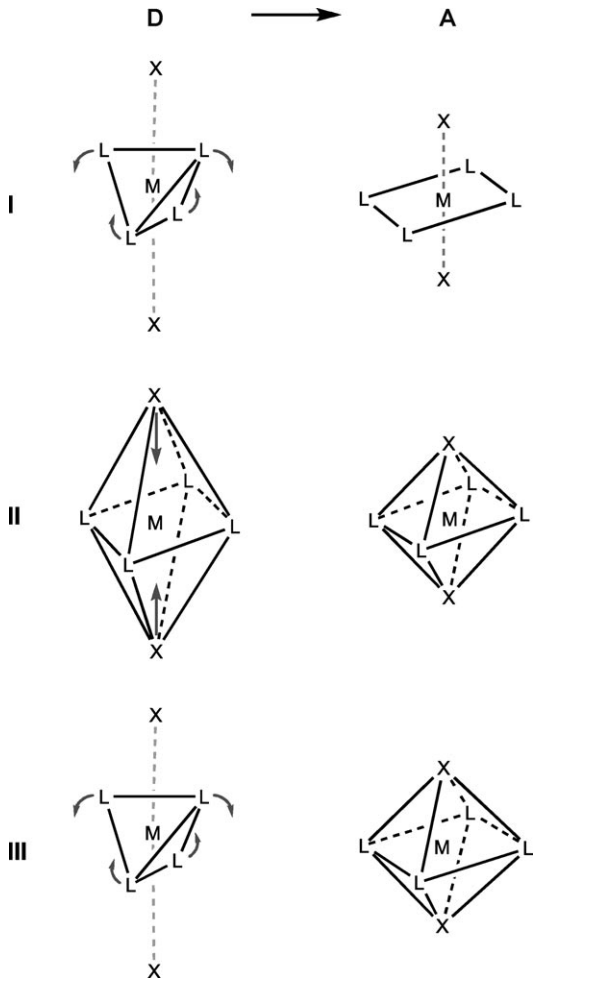

Figure 2. Types of association/dissociation pathways: **I**) the common fragment ML_n changes its shape from starting to end products; **II**) the common fragment ML_n retains its shape throughout the pathway; and **III**) two shapes with different number of vertices represent the end points of the reaction. The black lines indicate the ideal polyhedra **D** and **A** at the two extremes of the association/dissociation reaction in each case.

we can simply compare the shape measure of the common fragment ML_n with respect to that within the two ideal shapes **D** and **A**, whereupon we can calibrate its position along the minimal distortion pathway through the path-deviation function $\Delta_{\mathbf{D,A}}$ and the generalized interconversion coordinate $\varphi_{\mathbf{D\rightarrow A}}$. A first application of this approach to the description of the proton transfer from an ammonium cation to the $[Co(CO)_4]^-$ anion has been reported earlier.[24]

*Method **II**: The common fragment ML_n retains its shape throughout the pathway*: An example would be the association of two ligands to axial positions of a square-planar four-coordinate molecule to yield a *trans*-octahedral complex. In such a reaction, the ML_4 fragment remains square planar throughout (Figure 2, **II**). Under such circumstances, we are forced to compare the shape of all the participating atoms, ML_n and *m*X, with the fully associated and the fully dissociated (i.e., X atoms at infinite distance from the metal) systems. In the square-planar–octahedral example, this would mean considering as starting shape **D** of the path a square with two atoms at infinite distance, and an octahedron as the end shape **A**.

Although both approaches **I** and **II** can be implemented in a productive way, as will be shown below, there is a clear and important difference. In the common fragment approach, both **D** and **A** are attainable and we could in principle find structures at any distance between the two end points. In contrast, in the full-molecule approach, the real systems that we can structurally identify will have the entering ligands X at a finite distance from the metal within the crystal and, therefore, will never correspond to situations close to the reference shape of the initial dissociated system, with X at infinite distance. In such cases, therefore, the generalized coordinate loses its quantitative meaning and can be used only for comparative purposes.

*Method **III**: The molecular structure is compared with two polyhedra of different number of vertices*: We might define the path by two shapes with different numbers of vertices (Figure 2, **III**), but an analytical expression for the minimal distortion path in terms of shape measures is not known for those cases. For this approach to be applicable, the weakly bonded atoms X must be unequivocally identified.

*Method **IV**: There is loss and/or appearance of symmetry operations*: In some cases, the symmetry of either the common fragment or the composite change along the path, and we could use symmetry operation measures[28] instead of shape measures to locate the position of a given structure.

A first natural choice for the study of an association/dissociation path interconnecting two polyhedra with different number of vertices, ML_n and ML_nX_m, consists of plotting the shape measures of the structures relative to those two polyhedra along the path (method **III**). However, this approach requires the identification at each point along the path of the ligand or ligands for which the bonds to the metal atom are being formed or cleaved. This is what was done to analyze the S_N2 path for ligand substitution in $[SnXR_3]$ complexes through intermediate trigonal bipyramids $[SnXYR_3]$.[29] Such a strategy is a suitable one when a large number of structures along the path are known, but it has the disadvantage that no analytical expression has been derived to describe the minimal distortion association/dissociation paths as a function of $S_X(\mathbf{D})$ and $S_X(\mathbf{A})$. Method **I** has the advantage that the identification of the approaching ligands X is not required, and one can analyze only how the geometry of the common fragment reacts to the presence of unidentified nearby ligands. Another advantage of method **I** is that the minimal distortion path is fully defined and we can calibrate whether or not a given structure is on that path by making use of the path-deviation function $\Delta_{\mathbf{D,A}}(\mathbf{Q})$, as well as its position along the path through the generalized coordinate $\varphi_{\mathbf{D-A}}(\mathbf{Q})$. For that reason, we will use method **I** preferentially over strategy **III**. On the other hand, for those processes in which the geometry of the common fragment remains unaltered, method **I** cannot be applied and we must resort to methods **II** or **IV**.

Association/dissociation paths: from four to six: In this section we will consider three different pathways that can go from four to six coordination: 1) coordination of two ligands to axial positions of a square-planar complex, thus leading to a *trans*-associated octahedron, 2) approach of two ligands to faces of a tetrahedron to generate a *cis*-associated octahedron, and 3) coordination of two ligands to opposing edges of a tetrahedron to give a *trans*-associated octahedron.

From a square planar to a trans*-octahedral complex*: The well-known stereochemical behavior of six-coordinate Cu^{II} complexes that present significant elongation of two metal–ligand bonds in *trans* positions can be dealt with by comparing the structural data with the fully associated (octahedral) and fully dissociated (square planar with two ligands at infinite distance) extremes of the tetragonal distortion pathway. This strategy corresponds to case **II** (Figure 2), in which the two end points of the reaction pathway are an infinitely elongated tetragonal bipyramid **D** and a regular octahedron **A**. From the point of view of the shape measures, the fully dissociated extreme can be defined either by placing the two leaving ligands at distances at least 10^4 times the bond lengths, or by collapsing the four equatorial ligands to the position of the central atom.

In this study we have retrieved the structural data for all Cu^{II} complexes defined in the Cambridge Structural Database (CSD) as six coordinate (4877 structural data), together with those defined as four-coordinate with an approximately square-planar geometry and two contacts to donor atoms at the axial positions (1110 structural data). The results of the comparison of those structures with the regular octahedron (OC-6) and the fully dissociated tetragonal bipyramid are shown in Figure 3a. In that shape map, we see that most of the structures are close to the dissociation pathway, represented by the continuous line. Not unexpectedly, however, those structures are still far away from our ideal of

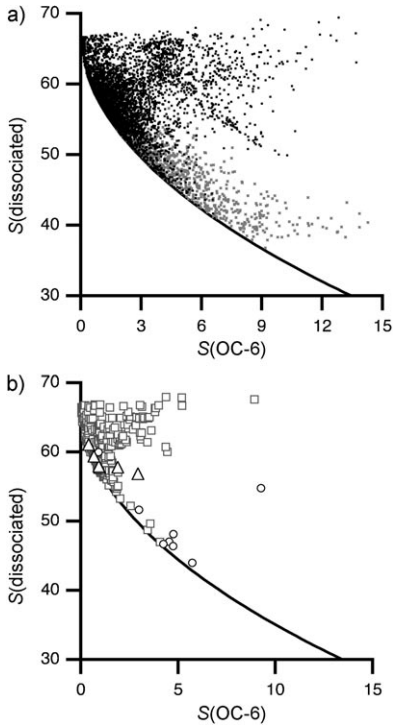

Figure 3. a) Octahedron to *trans*-dissociated shape map showing the structures of six-coordinated Cu^{II} complexes (■) and those of square-planar complexes with two contacts in axial directions within the 2.0–3.5 Å range (×), in which the continuous line represents the minimum distortion path. b) The corresponding map for Au^{II} (○) and Mn^{III} (□) six-coordinate complexes and for the solid-state compounds CrX_2 (X = F, Cl, Br, and I) and AgF_2 (△).

"full" dissociation, S(dissociated) = 0, which by definition can be reached only when the ligands are at an infinite distance from the metal. It is interesting to point out that some compounds classified as four-coordinate are closer to the octahedron than other complexes described as six-coordinate. This finding indicates how inconsistent we chemists are in assigning chemical bonds to a molecular structure, something we can live with, but that should not be ignored when discussing issues on chemical bonding. To show that a similar treatment can be applied to other Jahn–Teller active metal ions, we present also the dissociation map for six-coordinate Mn^{III} and Au^{II} compounds (Figure 3b), which also present a good number of structures nicely aligned along the dissociation path. Also shown in that map are some solid-state compounds of Jahn–Teller active metal ions, AgF_2 and CrX_2 (X = F, Cl, Br, I). From the position of many of those compounds along the dissociation path, it seems clear that a 4+2 coordination represents a better structural description than either a square planar or an octahedral coordination.

We must not forget that the shape measures are geometrical in nature, and different metal–ligand distances might appear in some cases due to the different atomic radii of the donor atoms involved. However, this caution applies only when comparing two structures that occupy not-too-distant positions along the dissociation path. The overall picture unmistakably shows a trend toward dissociation. A look at two of the "six-coordinate" compounds that appear closest to full dissociation illustrates this observation: $[Cu(py)_4I_2]$[30] (py = pyridine) and $[Cu(pyrazole)_4Br_2]$[31] have similarly high deviations from the octahedron (S(OC-6) = 6.66 and 6.50, respectively), and both appear exactly along the dissociation path (as indicated by zero values of the path-deviation function). Certainly, from those numerical values (corresponding to bond lengths of 3.46 and 3.37 Å, respectively) we cannot conclude that the Cu–I bonds have a degree of dissociation similar to the Cu–Br ones, but it is beyond doubt that the position of these compounds in the dissociation map indicates important degrees of bond dissociation in both cases. This assertion can be verified by noting that the "bond" distances exceed the sum of atomic radii[32] by 0.75 and 0.85 Å, respectively.

Another illustrative example of the pathway from the square to the octahedron is provided by the family of Ni^{II} compounds reported as square planar or octahedral. We have searched the CSD for six-coordinate Ni^{II} complexes, as well as for four-coordinate complexes with two contacts between Ni and two donor atoms at 3.0 Å or less. We have then selected those structures that deviate at most 5.2% from the ligand association/dissociation pathway (more information given in the Supporting Information), and plotted their shape measures relative to the octahedron and to a square-planar complex with two ligands at infinite distance (Figure 4a). The related solid-state compounds PdS_2 and $PdSe_2$ are also plotted in the same map for comparison. Some remarkable observations can be made by looking at the data represented in such a dissociation map:

1) There is a continuous distribution of six-coordinate structures from the regular octahedron (S(OC-6) = $\varphi_{OC\text{–}Dissoc.}$ = 0.00) to clearly dissociated complexes (S(OC-6) ≈ 15; $\varphi_{OC\text{–}Dissoc.}$ ≈ 45%) with, for example, Ni–O distances as long as 2.91 Å (Table 1), to be compared with an atomic radii sum[32] of 1.90 Å.
2) That distribution, however, is bimodal (Figure 4b), and two regions that correspond to six-coordinate complexes and four-coordinate complexes with two contacts from donor atoms to Ni are clearly identified.
3) Several compounds classified as square planar appear closer to the octahedron than many "octahedral" ones. Conversely, some complexes identified as octahedral present higher degrees of dissociation than many assumed to be square planar.
4) All compounds with two contacts at less than 3.1 Å form nearly linear X-Ni-X bond angles (average 176 (7)°).
5) In practically all compounds with two contacts at up to 3.8 Å, the NiL_4 fragment is square planar to a very good approximation (S(SP-4) ≤ 2.2 for more than 1200 structural data sets). The only exception is a complex[33] in which the Ni atom can be considered neither square planar (S(SP-4) = 6.73) nor tetrahedral (S(T-4) = 14.41), but as a sawhorse or seesaw with a short contact (2.46 Å)

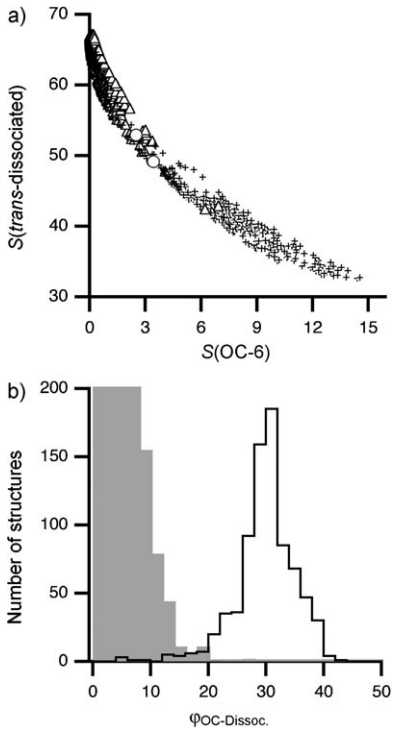

Figure 4. a) Portion of a shape map with the structures of Ni^{II} complexes that deviate at most 5.2% from the minimal distortion path from octahedral to square planar with two *trans* ligands dissociated. Triangles correspond to compounds codified in the CSD as six-coordinate, and crosses correspond to four-coordinate compounds with contacts from two donor atoms to Ni at 3.8 Å or less, and which form an X···Ni···X angle larger than 160°. The solid-state compounds PdS_2 and $PdSe_2$ are also shown (○). b) Histogram showing the distribution of compounds labeled as six-coordinate (gray bars) and four-coordinate with two contacts (white bars) as a function of the generalized coordinate for the same path.

to an oxygen atom of a polyoxotungstate anion, thus giving an effective 4+1 coordination with a second contact at a much longer distance (3.30 Å). Therefore, there is no structural evidence of *trans* association to tetrahedral Ni^{II} ions on the way to the octahedron.

We suspect that Ni^{II} complexes encoded as square planar that have octahedral shape measures smaller than 2.0 would be better described as octahedral than as square planar. The difficulty in the assignment of square planar or octahedral geometry has permeated into the literature. In $[Ni(bipy)_2(H_2O)_2]SO_4$ (bipy = bipyridine; ABPYNI entry, Table 1),[34] for instance, the nickel atom is classified as four-coordinate in the CSD, but the original paper described this structure in a more ambiguous way as a notably deformed octahedron. In a {Ni(macrocycle)$(SCN)_2$} unit within a chain compound (WUCCIG, Table 1), the coordination geometry has been described[35] as a "prolate octahedron," although the shape measures analysis suggests practically a four-coordinate situation. The nickel atom in $[Ni(en)_2](NO_3)_2$ (en = ethylenediamine; FAXLUM, Table 1) is described[11] as a "tetragonally distorted octahedron" with an O atom of the nitrate counterion presenting a "semicoordinating" interaction. In this regard, we must stress that all "square-planar" complexes with Ni–O "contact" distances (Table 1) well within the range of the standard bond lengths for octahedral complexes (Table 2) present generalized dissociation coordinates of less than 10%.

A word of caution must be said at this point, however, as done above for copper compounds; it regards the intrinsic differences in bond lengths attributable to donor atoms of significantly different size. In $[Ni([14]ane\text{-}S_4)]BF_4$ (TTCDNI, Table 1)[36] and the perchlorate of a related macrocyclic complex (MAXSOT, Table 1),[37] moderate deviations from the octahedral shape result from relatively small differences between the bonded Ni–S distances (2.18 Å) and the nonbonded contacts between the Ni atom and the BF_4^- (Ni–F = 2.8 Å) or ClO_4^- (Ni–O = 2.97 Å) counterions.

An important question arises when one looks at the continuum of coordination of two *trans* ligands, from strongly bound to neatly dissociated. Since square-planar Ni^{II} complexes are diamagnetic (spin = 0) but octahedral ones are paramagnetic (spin = 1), one should expect a spin crossover along the dissociation/association pathway. We are not aware of the existence of a general study on this issue. Although it would constitute an exciting research topic, it will encounter difficulties, because in many instances the magnetic behavior has gone unreported, and often the high- or low-spin nature of a complex is deduced from interatomic distance criteria without magnetic or spectral evidence.[37] Nevertheless, our shape analysis has allowed us to identify cases of significantly dissociated octahedra for which a low-spin behavior has been reported (see entries PTOCNI10[38] and LATXOU[39] in Table 1).

From tetrahedral to cis *octahedral*: Brownmillerite, Ca_2AlFeO_5, has attracted much interest because it is one of the components of ordinary portland cement. In its structure, the tetrahedral Al site can be more or less distorted, whereas two nearby oxygen atoms establish Al···O contacts, thus describing a pathway from the tetrahedron to the octahedron with the two incoming ligands occupying *cis* positions (Scheme 2). To analyze structures along this path, we consider the extremes of the reaction to be the regular tetrahedron (T-4) and the ML_4 seesaw (SS-4) fragment within the octahedral $[MX_2L_4]$ complex formed, thus adopting strategy **I**. The structures of several compounds found to be along this pathway are plotted in a shape map relative to the tetrahedron (T-4) and the sawhorse (SS-4) reference shapes in Figure 5.

Among the structures that provide still pictures of such a ligand association path (Figure 5) we have found the series of substitutional solid solutions $Sr_{2-x}Ba_xCo_2O_5$ ($0.00 \le x \le 0.59$),[40] even if with only small changes in coordination geometry, $Ca_2Fe_2O_5$,[41] $Ca_2Fe_{2-x}Al_xO_5$ ($0 \le x \le 0.59$; at larger Al contents there is a phase change with octahedral coordination),[40] $Ca_{1.6}Fe_{1.63}Al_{0.37}O_5$ at variable pressure,[41] and $LnSrCuGaO_5$ (Ln = La, Pr, Nd).[42] The octahedral extreme of the pathway is represented by the structure of $Sr_{1.6}Ba_{0.4}Co_2O_5$ at a temperature of 940°C (rightmost point

Table 1. Generalized coordinates along the *trans*-dissociation path (see Figure 4a, for reference) for some structures of Ni^{II} complexes classified in the CSD as four-coordinated with two contacts from X groups at less than 3.0 Å, compared with structures of complexes classified as six-coordinated.

Refcode	Δ [%][a]	$\varphi_{OC-Dissoc.}$	X	d [Å][b]	δ [Å][c]	CN[d]
MIPZNI10	2	4.9	ClO_4^-	2.20	0.30	4
PELCOZ	3	5.1	H_2O	2.13, 2.20	0.23, 0.30	4
ABPYNI	4	6.3	SO_4^{2-}	2.15	0.25	4 (4+2)
POHBUK (Ni2)	7	8.9	N_3^-	2.10, 2.29	0.15, 0.34	6
POHBUK (Ni1)	7	9.2	N_3^-	2.11, 2.29	0.16, 0.34	6
MIPZNI01	1	9.8	ClO_4^-	2.42	0.52	4
GETVIL	0	12.4	NO_3^-	2.58	0.68	4 (4)
FAXLUM	1	13.0	NO_3^-	2.55	0.65	4 (4+2)
WEJLED (Ni1)	0	13.5	N_3^-	2.63	0.68	4
OHODIY	1	13.8	O^{2-}	2.59	0.69	6
BZIMNI	1	14.0	Cl^-	2.42, 2.94	0.16, 0.68	6
REFTOM	1	14.0	ClO_4^-	2.49, 2.58	0.59, 0.68	4 (4)
XILXIA	1	14.6	H_2O	2.52	0.62	6 (6)
WEJLED (Ni2)	0	15.0	N_3^-	2.69	0.74	4
WOCBOF	1	15.4	AcO^-	2.70	0.80	6
TTCDNI	2	16.4	BF_4^-	2.89	1.08	4
RAMQUS	2	16.6	ClO_4^-	2.57	0.67	6
MAXSOT	1	17.2	ClO_4^-	2.97	1.07	4
JIGTIC	0	17.7	S (trimer)	3.05	0.76	6
PTOCNI10	4	18.2	S-macrocycle	2.94	0.65	6 (4+2)
LATXOU	1	19.3	Br^-	2.91	0.47	6
CEBJID	1	21.3	ClO_4^-	2.88, 2.91	0.98, 1.01	6 (4)
WUCCIG	0	26.4	SCN^-	3.18	0.89	6
IVOMOV	2	27.9	$S_2(POR)_2^{2-}$	3.22	0.93	6

[a] Δ is the value of the path-deviation function. [b] d is the Ni···X distance. [c] δ is the difference between the Ni–X distance and the sum of atomic radii. [d] Under the heading "CN," we indicate the coordination number assigned in the CSD and that given by the authors in the original structural report (in parentheses).

Table 2. Average bond lengths to octahedral Ni (estimated standard deviations in parentheses) of some coordinated ligands. N is the number of structural data found.

Ligand	Ni–X [Å]	N
NO_3^-	2.10 (6)	148
ClO_4^-	2.28 (12)	48
SO_4^{2-}	2.07 (4)	78
N_3^-	2.11 (5)	232
Cl^-	2.45 (10)	495
H_2O	2.08 (5)	2265
SCN^-	2.56 (11)	62

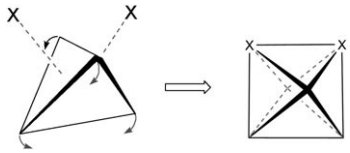

Scheme 2.

in Figure 5a).[43] Let us stress that even if an applied pressure seems to have a small effect, it is clearly along the tetrahedral to *cis*-octahedral pathway as seen in Figure 5b for $Ca_2Fe_2O_5$ and $Ca_{1.6}Fe_{1.63}Al_{0.37}O_5$,[41] with the higher pressures favoring the higher coordination number.

The same path is covered in part by the B atoms in the family of ABX_4 compounds with the $NiWO_4$ structure, as can be seen in the shape map (Figure 5a). In the case of pseudobrookite, $FeTi_2O_5$, the coordination sphere of Ti can also be approximately described as being along the tetrahedral to *cis*-octahedral pathway, even if it shows a relatively high deviation from the path (21%). That behavior is in contrast with the *trans* association pathway from the tetrahedron to the octahedron that is showcased by Ti in anatase (Figure 1).

In the molecular world, we can also find examples of structures that fall along this path. On one hand, in two homoleptic organometallic complexes of formula $[M(C_6Cl_5)_4]$ ($M = Pt^{IV}$, Rh^{III})[44] two *ortho*-Cl atoms of σ-bonded pentachlorophenyl ligands form secondary interactions with the metal atoms, thus completing a nearly octahedral coordination (95–96% along the tetrahedral to *cis*-octahedral pathway). Other examples that have not gone as far towards the octahedron correspond to a silver complex reported by Jalón and co-workers[45] (52%) and the Zn complex[4] mentioned in the Introduction (37%).

From tetrahedral to trans *octahedral*: To analyze the structures of titanium dioxide and titanates discussed in the Introduction (Figure 1), we can use the same approach (**I**) as in the previous section, but defining now the tetrahedron and the square as ideal shapes at the two extremes of the reaction pathway. While the coordination of Ti in rutile is very close to octahedral, such that the common TiO_4 fragment has $S(SP\text{-}4) = 0.52$, and nearly perfectly tetrahedral in the barium titanate, with $S(T\text{-}4) = 0.07$, in anatase it is a distorted tetrahedron, exactly along the minimal distortion pathway with a generalized coordinate for conversion to the square-planar fragment of the octahedron $\varphi_{T\rightarrow SP} = 34\%$. A related situation appears for the Group 14 elements[46] in the β-Sn structure, found also for high-pressure forms of Si, Ge, and Sr,[47] with similar partial conversions from the tetrahedral to octahedral coordination geometry measured by generalized coordinates $\varphi_{T\rightarrow SP} \approx 56\%$.

From two to six: A formal two-coordination with four additional contacts en route to an octahedron (Scheme 3) is a reasonable description for the structure of β-HgO_2.[48] Since a linear dicoordinate HgO_2 unit retains its geometry throughout the process of simultaneous association of four ligands, we resort to method **II**. The starting point, the linear

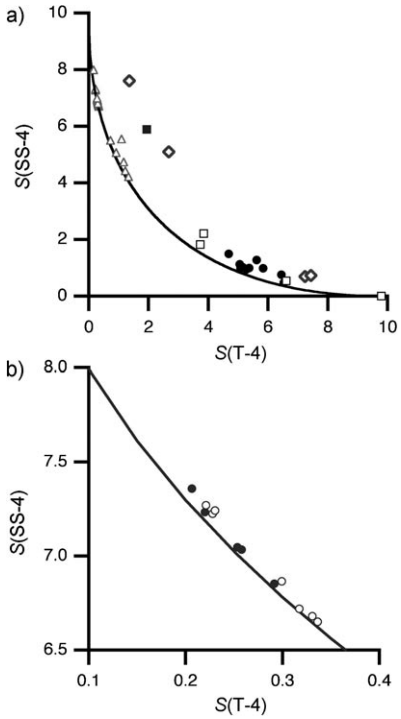

Figure 5. a) Coordination geometries of the atom at the Al site in the brownmillerite Ca_2FeAlO_5 structure, plotted in a tetrahedron/seesaw map, for $Ca_2Fe_2O_5$ at various pressures, $Ca_2Fe_{2-x}Al_xO_5$ ($0 \le x \le 0.59$) and $LnSrCuGaO_5$ (△); for $Sr_{1.6}Ba_{0.4}Co_2O_5$ at different temperatures (□), for compounds with the $NiWO_4$ structure (●), pseudobrookite $FeTi_2O_5$ (■) and molecular complexes mentioned in the text (◇). b) Detail of the nearly tetrahedral region of the same shape map showing the structures of $Ca_2Fe_2O_5$ (●) and $Ca_{1.6}Fe_{1.63}Al_{0.37}O_5$ (○) at different pressures.

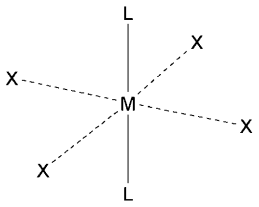

Scheme 3.

ML_2 complex, is therefore represented by a "six-coordinate" tetragonal $[ML_2X_4]$ complex in which four equatorial X ligands are at infinite distance from the central atom (which is equivalent to considering two ligands collapsed at the center of the molecule and four equatorial ligands at finite distances). We find that the structure of β-HgO_2 deviates by a negligible amount from that path; it has an octahedral shape measure of only 1.64, which indicates that it is better described as a compressed octahedron than as a linear molecule. Secondary coordination of four ligands to linear organomercurial fragments has also been noted.[49]

It is precisely the compressed octahedron that has been such a controversial issue in Cu^{II} chemistry. The Jahn–Teller effect is known to act on six-coordinate Cu^{II} centers mostly through a tetragonal elongation distortion that results in two long and four short copper–ligand distances. There have been, however, several reports of supposedly "compressed" copper complexes (i.e., with four long and two short bond lengths) that in many instances were shown later to be an artifact resulting from static or dynamic disorder, as verified by EPR spectroscopy or extended X-ray absorption fine structure (EXAFS) experiments.[50] This has led Halcrow to qualify those compressed octahedra as a "structural chimera."[51] Nevertheless, there seems to be a well-characterized case in which the designed ligands used force the compression distortion instead of the more usual elongation one.[51]

The questions we then ask ourselves are: Can we describe the inverted Jahn–Teller distortion, real or artifactual, by means of shape measures? Can we tell elongation from compression distortions of the octahedron? The answer is: Yes, we can! We faced a difficult problem, though, because the numerical values of the shape measures relative to three reference figures (the regular octahedron, a fully dissociated version, and a fully compressed version) are not informative by themselves and do not allow us to identify an elongation from a compression of the octahedron. However, by analyzing the ideal dissociation and compression pathways, we found that the difference between the shape measures relative to the two fully distorted octahedra, $\rho = S(\text{dissociation}) - S(\text{compression})$, can be successfully used as a discriminating parameter. For the perfect octahedron, $\rho = 33.33$, and larger values are therefore indicative of an inverted Jahn–Teller distortion. We have therefore developed a specific shape map for tetragonal Jahn–Teller distortions by plotting ρ as a function of the octahedral shape measure (Figure 6, continuous lines). In that map, the lower line represents the elongation and the upper branch the compression distortion.

We also show in the new map (Figure 6) the plethora of Cu^{II} complexes with N- or O-donor ligands (4224 crystallographically independent data sets found). Among them, all those with ρ larger than 34.0 are found to effectively present

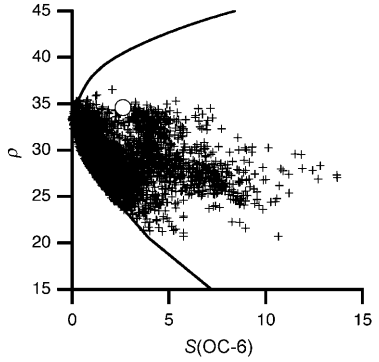

Figure 6. Map of six-coordinated Cu^{II} complexes with N- or O-donor ligands relative to the regular octahedron (OC-6), and the parameter $\rho = S(\text{dissociated}) - S(\text{compressed})$ (with two and four ligands at infinite distance, respectively). The upper branch corresponds to the compression, the lower one to the elongation pathway. The data for the solid-state compound $KAlCuF_6$ are also shown (○).

four long and two short copper–ligand distances (data provided in the Supporting Information). It must be stressed that the present analysis does not tell us whether those structures correspond to genuine inverted Jahn–Teller distortions or not. Interestingly, among three compounds in which tridentate ligands impose an unambiguous compressed tetragonal bipyramid,[52,53] the ρ value is clearly discriminating in two cases (34.7 and 34.5),[52] but inconclusive in the other (32.6),[53] because severe bond-angle distortions place that compound away from the pure tetragonal compression path.

Among the solid-state compounds that have been qualified as genuinely compressed octahedra, $KAlCuF_6$ has been found by us to have $\rho = 34.1$, which is consistent with its having two short and four long Cu–F bond lengths. However, we will see below that the Cu atom in this compound presents clear signs of being quasi-seven-coordinated.

From six to seven: Potentially heptadentate ligands of types **1** and **2** appear in several metal complexes with the apical nitrogen atom at distances ranging from clearly bonding

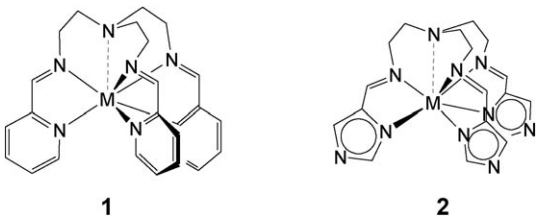

1 **2**

(2.50 Å) to nonbonding (3.92 Å). When the apical nitrogen is at a short distance, the metal is heptacoordinated and its coordination sphere defines a capped octahedron (CO-7).[54] When not bonded, the metal environment becomes octahedral (OC-6). Many compounds, however, present intermediate situations in which the coordination number is ill-defined. This can be seen by plotting the shape measures *S*(CO-7) and *S*(OC-6) of the MN_6 and MN_7 fragments, respectively, as a function of the apical M–N distance (Figure 7). The best examples of the capped octahedral geometry are those of Fe^{II},[55] Mn^{II},[56] and Fe^{III} complexes.[57] Even when formally six-coordinated, the structures of transition-metal compounds with ligands that belong to this family map the initial steps of the path from the octahedron to the capped octahedron.

A particularly interesting system is the spin-crossover complex ion[58] $[Fe(\mathbf{1})]^{2+}$, which shows a significant variation in the distance of the tertiary nitrogen atom to Fe with varying temperature.[59] However, no change in coordination number has been claimed in this case, because in the high-spin state such a distance is still too large (3.21 Å) to consider an Fe–N bond, and only "a reorganization of the coordination environment of the iron ion toward a more regular octahedron" was identified upon transformation of the high-spin to the low-spin state. Given the evidence put forward by Figure 7 that those structures are along the interconversion pathway between the octahedron and the capped octahedron, we have submitted the variable-temperature structural data reported by Gütlich and co-workers to a shape analysis relative to that dissociation path. The shape measures (Figure 8) clearly show that the spin transition at

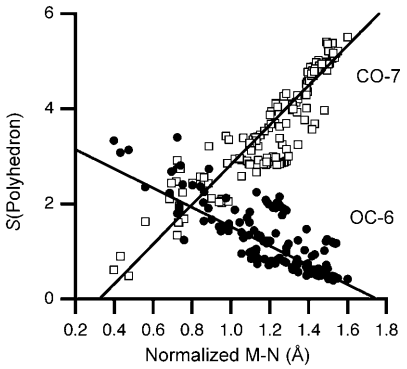

Figure 7. Shape measures of the MN_6 and MN_7 atom sets in complexes with ligands **1** or **2**, relative to the octahedron (OC-6, ●) and capped octahedron (CO-7, □), respectively, as a function of the difference of the apical M–N distance and the sum of the atomic radii.

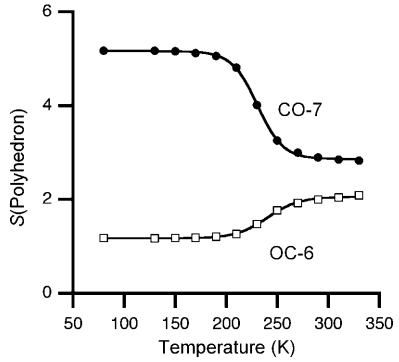

Figure 8. Shape measures for the spin-crossover ion[59] $[Fe(\mathbf{1})]^{2+}$ as a function of the temperature.

around 250 K is associated to a sharp change in geometry, from nearly octahedral at low temperatures (low-spin state) to a geometry intermediate between the octahedron and the capped octahedron at high temperatures (high-spin state). In contrast, the analogous Zn complex retains an intermediate geometry all the way from 95 K to room temperature ($1.9 \leq S(\text{OC-6}) \leq 2.0$).

Another remarkable pentadentate ligand, **3**, forms a variety of Mn^{II} and Fe^{II} complexes.[20,60] All those complexes appear as well-defined seven-coordinated pentagonal bipyramids (PBPY-7), with corresponding shape measures smaller than 0.3 (Scheme 4). The only exception is an Fe^{II} compound at low temperature,[19] at which one of the ether groups partially dissociates from the ligand, simultaneously to a spin-crossover transition. In that case, the increase of the pentagonal bipyramidal measure and the decrease in the octahedral measure both indicate that the structure is practi-

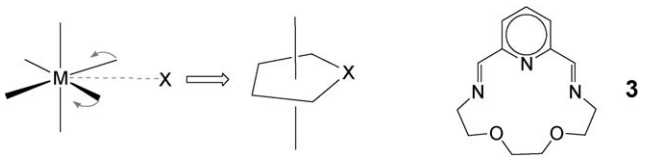

3

Scheme 4.

cally intermediate between those two ideal shapes (Figure 9).

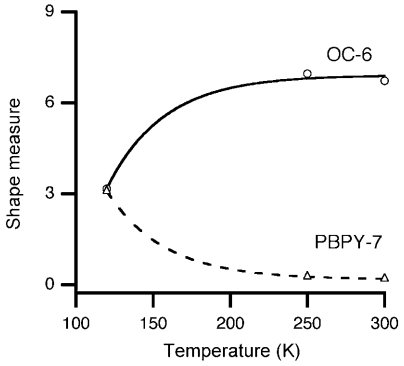

Figure 9. Variation with temperature of the octahedral (OC-6) and pentagonal bipyramidal (PBPY-7) measures in a spin-crossover Fe^{II} compound with ligand **3**.[19]

The coordination sphere of Ta in Ta_2O_5 is found to be on the same pathway that connects the octahedron and the pentagonal bipyramid, with $\phi_{vPBPY\rightarrow OC}=71\,\%$, in which vPBPY stands for a pentagonal bipyramid with a vacant equatorial site. The coordination sphere of the copper atom in a quite different compound, $KCuAlF_6$, is also intermediate between the octahedron and the pentagonal bipyramid. The various compounds with this structure[61] span a large part of the octahedron to pentagonal bipyramid path (Figure 10), as seen in the corresponding dissociation/association map in which the structural data for the persistent ML_6 fragment has been plotted (method **I**).

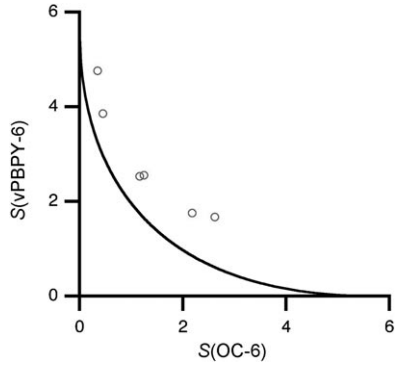

Figure 10. Shape map for the association of a ligand to an octahedron to yield a pentagonal bipyramid, in which the structural data for the family of compounds with the $KCuAlF_6$ structure is seen to approximately follow the minimal distortion path (continuous line).

From four to seven: We have identified a pathway that goes from a tetrahedron to a capped octahedron through the simultaneous approach of three incoming ligands (Scheme 5).

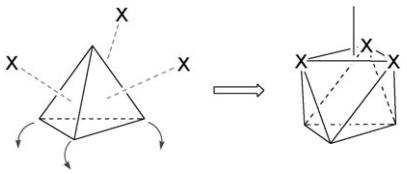

Scheme 5.

A representative example of a metal atom found along that pathway is Al in $Mg(AlH_4)_2$, the structure of which has been solved at several temperatures between 8 and 295 K.[62,63] The structural data represented in a shape map relative to the tetrahedron and the tri-vacant capped octahedron (Figure 11) show that there is a significant approach to a

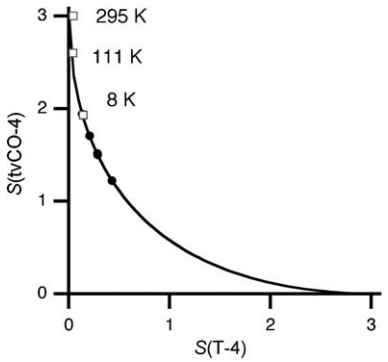

Figure 11. Shape map for the association of three ligands through faces of a tetrahedron (T-4) on its way to a trivacant capped octahedral (tvCO-4) geometry, in which we plot the data for $Mg(AlH_4)_2$ at different temperatures[62] (□) and for the A site in several compounds with the $A_2M_3O_8$ nolandite structure (●). The data shown come from $Zn_2MoW_2O_8$, $Fe_2Mo_3O_8$, $Mg_2Mo_3O_8$, $ScZnMo_3O_8$, and $Zn_2Mo_3O_8$.

capped octahedron of hydride ions around Al as the temperature is lowered. One of the A atoms in compounds with the $A_2M_3O_8$ nolandite structure is also along the pathway that goes from the tetrahedron to the capped octahedron. In $Zr(MoO_4)_2$,[64] with the same structural type as $Mg(AlH_4)_2$, the Mo atom is practically unperturbed from the tetrahedral geometry, even if there are also three Mo···O contacts through face centers (3.48 Å).

From four to eight: Three different pathways have been identified for the simultaneous association of four ligands to a four-coordinated metal center. These pathways lead to the triangular dodecahedron, the gyrobifastigium, and the cube, respectively (see Pathways D_{2d}, D_2, and D_{2h} in Scheme 6). The compounds with $La_2(WO_4)_3$ and UCl_4 structures represent two different steps along pathway D_{2d} in Scheme 6. In the former, the atoms occupying the W site are nearly tetrahedral, but small distortions along the spread pathway that

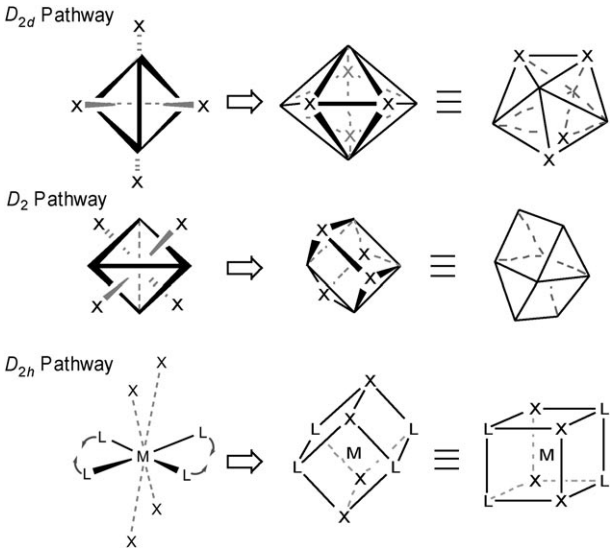

Scheme 6.

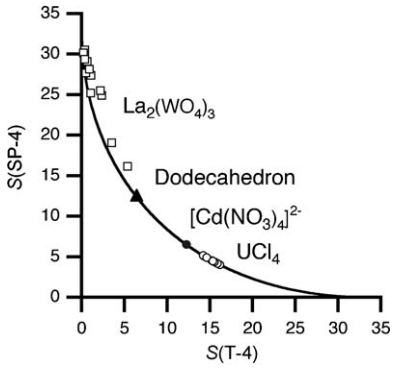

Figure 12. Shape map for the tetrahedron–square-planar rearrangements of the types shown in D_{2d} and D_2 Pathways in Scheme 6, in which structural data for the donor atoms at short distances in compounds with the $La_2(WO_4)_3$ (W site, □) and UCl_4 (U site, ○) structures are plotted. The triangle indicates the position of the equatorial set of ligands in the reference triangular dodecahedron, and the filled circle the CdO_4 group with short Cd–O distances in the $[Cd(NO_3)_4]^{2-}$ anion.

goes to the square-planar geometry can be associated to the presence of four contacts from donor atoms at longer distances through the centers of the tetrahedral faces. The most notorious effect is seen for the W atoms in $[Dy_2(WO_4)_3]$,[65] for which the presence of four oxygen atoms at quite long distances is combined with O-W-O bond angles as large as 129°. Those structures have D_{2d} symmetry, thus indicating that the coordination pathway is the one shown in Scheme 6, which leads to the eight-vertex triangular dodecahedron.[66] Since the four coordinated atoms with tetrahedral bond angles are converted in such a pathway to a flattened tetrahedral portion of the dodecahedron with conventional angles of 139°, we could extrapolate to a final regular square as the destination shape. Therefore, by adopting method **I**, we can plot the structural data for the strongly bonded O atoms in these compounds on a tetrahedron–square shape map (Figure 12). The structural data is seen to nicely cover the path between the tetrahedron and the dodecahedron

Another family that presents a 4+4 coordination of the type generated by the D_{2d} pathway (Scheme 6) is that of the four-valent rare-earth halides that crystallize in the UCl_4 structure. In these compounds, the ligand association has gone much farther than in the lanthanum tungstate family, slightly beyond the reference triangular dodecahedron in the degree of planarization of their equatorial ligands (Figure 12). We should not be surprised by this behavior, since the corresponding bond angles are as high as 154° (in $NpCl_4$), and the criterion of ideality for the triangular dodecahedron is not unequivocally defined by symmetry but adopted by convention.

Interestingly, an anionic $[Cd(NO_3)_4]^{2-}$ complex[67] presents a related type of secondary coordination. Each of the nitrate ions in that complex is strongly coordinated through one oxygen atom (2.295 Å), and weakly coordinated (2.576 Å) through a second oxygen atom. The whole arrangement has D_2 symmetry, which corresponds to an approach of the weakly bound ligands off the center of the tetrahedral faces (sketched in the D_2 pathway, Scheme 6), and can be described as being along the path from the tetrahedron to the gyrobifastigium,[66,68] in which the four bonded atoms form the equatorial square. Such a pathway can thus be analyzed by means of the four strongly bonded ligands (method **I**) that would rearrange from tetrahedral to square planar upon association of the four entering ligands, the same fragments used for the analysis of the conversion of the tetrahedron into a triangular dodecahedron. The structure of this cadmium complex falls right along that path at 58% of its total way toward the gyrobifastigium. Indeed, in spite of the significant differences in Cd–O bond lengths to the two sets of oxygen atoms and its relatively large shape measure of *S*(GBF-8) = 4.39, it has been shown that the best description of the Cd coordination sphere in this complex is provided by the gyrobifastigium.[66]

A third situation intermediate between four- and eight-coordination is found in the central Pd atom of a Pd_{13} cluster reported recently.[69] Its coordination sphere can be described as being midway between square planar and cubic (D_{2h} pathway, Scheme 6) by looking only at the persistent ligands that evolve from a square to the rectangle that corresponds to a diagonal plane of the coordination cube. That structure shows a negligible deviation from the minimal distortion path and is practically midway between the two extremes ($\varphi_{SP\rightarrow tvCU} = 48\%$, in which tvCU stands for a tetravacant cube).

From six to eight: Compounds as diverse as GeO_2, SnO_2, SiO_2, RuO_2, and MgF_2 (the latter at pressures above 14 GPa)[70] present the low-temperature PdF_2 structure, in which the metal atom occupies an octahedral coordination site. However, the octahedron shows in all cases small but significant distortions (octahedral shape measures 0.95–1.24) that converts it into a compressed trigonal anti-

prism with O-M-O bond angles as large as 99°. A close inspection indicates that in all those structures two anions make contacts to the metal atom along the trigonal axis, as is the case for GeO_2. The approach of two ligands in this geometry, described earlier as a "bicapped flattened octahedron"[71] could be ascribed to an association pathway that would ultimately convert the octahedron into a hexagonal bipyramid (Scheme 7), in which the initial six-coordinate

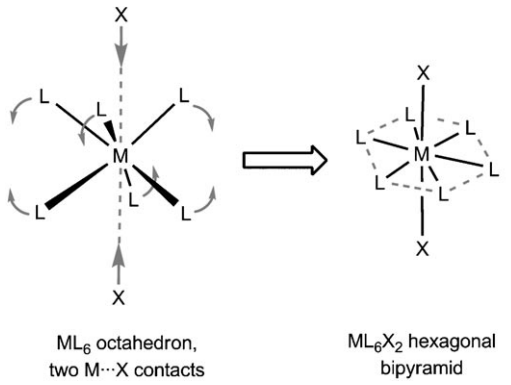

Scheme 7.

group becomes the basis of the bipyramid. In spite of the relatively long distances of these contacts, they seem to be correlated with the degree of distortion of the octahedron, and the structural data for the six-coordinate fragment is nicely aligned along the octahedron–hexagon path, as seen in a detail of the shape map (Figure 13a).

A much stronger distortion along the same pathway is found for the Hf1 atom of $Ca_6Hf_{19}O_{44}$, with a coordination clearly intermediate between six-coordinate octahedral and eight-coordinate hexagonal bipyramidal ($\varphi_{OC\rightarrow Hex}=46\,\%$). In Figure 13b we can see its situation in the same ligand association pathway as the PdF_2 structures. For comparison, we show there also the corresponding data for the family of fully eight coordinate complexes with hexagonal bipyramidal geometry supported by a hexadentate crown ether,[66] as well as those of complexes with potentially octadentate octaaza-sepulchrate ligands,[72] for which the two apical nitrogen atoms, even if loosely bound, are felt by the metal atoms that present non-negligible distortions from octahedral coordination (Figure 13b).

Another possible path for the simultaneous association of two ligands to the octahedron, represented in Scheme 8, leads to the cube. A realization of that pathway may be found in the ABX_4 compounds with the $NiWO_4$ or $YbTaO_4$ structures, which comprise $CoMoO_4$, $NaErCl_4$, $MnReO_4$, MWO_4 (M = Mg, Mn, Fe), $MNbO_4$ (M = In, Re), and $MTaO_4$ (M = In, Nd, Sm, Gd, Dy, Ho, Er, Tm, Yb, Lu). In that structure, the B site of which has been shown above to approach hexacoordination from the tetrahedron (Figure 5), two additional ligands at still longer distances describe the path to octacoordination. In Figure 14 we show those structures in the shape map relative to the octahedron and a di-

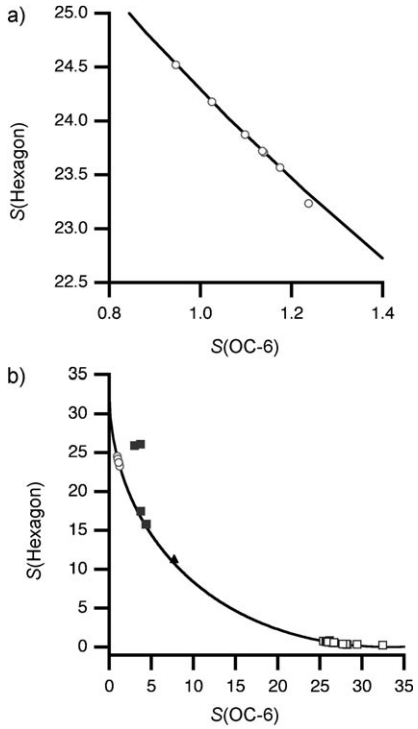

Figure 13. a) Structural data for compounds of the PdF_2 family (○) plotted in the hexagon versus octahedron shape map. The continuous line represents the minimal distortion pathway in Scheme 7. b) The same data is shown on a wider scale on the map for the full pathway, together with those of the Hf atom in $Ca_6Hf_{19}O_{44}$ (▲), and the metal atoms in the [M(crown-6)L_2] (□) and octaaza-sepulchrate complexes (■).

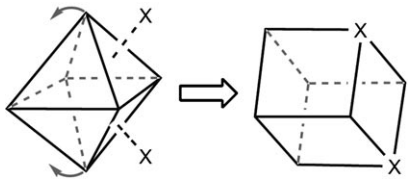

Scheme 8.

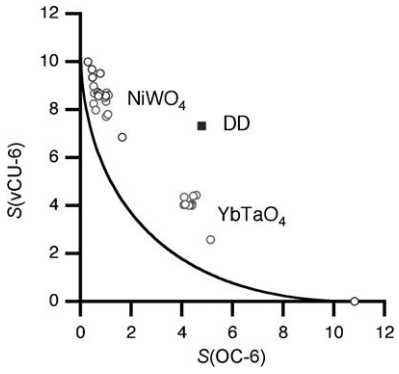

Figure 14. Stereochemical data for the atoms at the W site in compounds with the $NiWO_4$ structure, and for those at the Ta site in compounds with the $YbTaO_4$ structure, plotted in an octahedron-divacant cube association/dissociation map.

vacant cube, which results from an approach of two ligands to neighboring faces of an octahedron (Scheme 8). It must be noted, however, that these structures present a significant deviation from the ideal path, a fact that can be attributed to the incomplete coordination of two of the six ligands of the purported octahedron. Thus, these compounds could probably be best described as having a 4+2+2 coordination, with Ta−O distances of 2.08, 2.27, and 2.97 Å.

Symmetry maps for association/dissociation paths: To complete our survey of the possibilities of describing association/dissociation paths by means of shape and symmetry measures, we revisit two of the families discussed above in terms of shape measures, analyzed now from the point of view of their symmetry operation measures[28] (method **IV**). The first case we consider is the conversion of a tetrahedron into a *cis*-octahedron (see Scheme 2). It is advisable to analyze symmetry operations that are present at one end of the pathway and absent at the other end, in such a way as to have a monotonous dependence of the symmetry operation measures on the reaction coordinate. Thus, for the tetrahedron–octahedron pathway we have chosen the fourfold rotation and an inversion center. Structures along this path should therefore present large values of both $Z(C_4)$ and Z(inversion) at the early stages of the association process and decrease down to zero as the octahedron is formed. The path is not univocally defined because the correlation between the contact distances and the angular distortion of the ML_4 fragment is not known a priori and may vary from one system to another.

The structural data for the family of $NiWO_4$ compounds (Figure 15) are seen to meet our qualitative expectations, with both $Z(C_4)$ and Z(inversion) decreasing simultaneously (but more so the inversion than the rotation measure) as the coordination polyhedron approaches the octahedron. It must be noticed that the structures follow a symmetry path (Figure 15) more closely than the minimal distortion path (Figure 5). This is because different combinations of bond angles and contact distances may have the same symmetry contents. In other words, we find again that shape is a more stringent criterion than symmetry.[1]

For the other path we analyze here, the association of two ligands to *trans* faces of an octahedron to yield a hexagonal bipyramid (Scheme 7), we expect a loss of the fourfold rotation of the octahedron with the simultaneous appearance of the sixfold rotation of the bipyramid. The family of compounds with the PdF_2 structures, discussed above in terms of shape measures, shows nicely the gradual symmetry changes (Figure 15b), even if they are still relatively far from the two ideal symmetries. In this case, comparison of Figure 15b and Figure 13a shows that the structures follow a pathway that is both of minimal distortion and maximal symmetry.

A summary of the variety of association/dissociation paths analyzed in this paper is presented in Table 3; the method used is specified as well as the main families of compounds taken as examples.

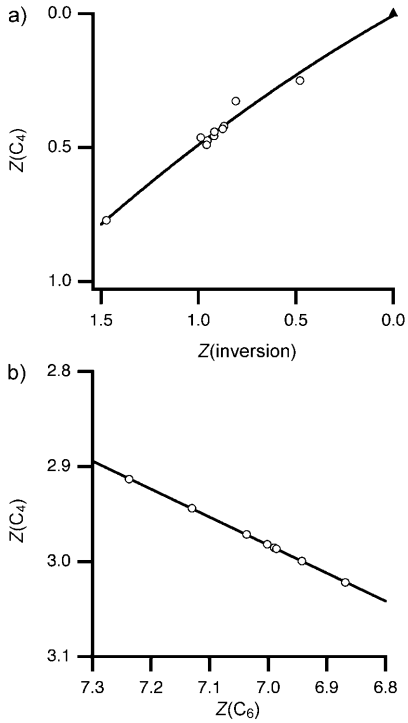

Figure 15. a) Symmetry operation measures for the family of $NiWO_4$ compounds (○) relative to a C_4 rotation and an inversion, which describes the association pathway given in Scheme 2. The triangle represents the ideal octahedron, whereas the coordinates of the ideal tetrahedron with two additional ligands at infinite distance are (35.18 and 15.78). b) Symmetry map for the conversion of an octahedron with two contacts on *trans* faces to a hexagonal bipyramid (see Scheme 7), using structural data for a family of PdF_2 structures (○). The lines are included as a guide to the eye.

Conclusion

We have shown that shape and symmetry operation measures allow for an accurate stereochemical description of coordination geometries that do not correspond to a well-defined coordination number. Those structures, be they theoretically derived or experimentally determined, can in many instances be seen as snapshots along a ligand association (or, conversely, dissociation) pathway.

Four alternative approaches (**I**–**IV**) have been defined that make use of continuous shape (**I**–**III**) or symmetry operation (**IV**) measures. Using shape measures, the polyhedral rearrangement attendant on association/dissociation processes can be best analyzed by taking as end points of the reaction pathway two polyhedra with the same number of vertices. One can then focus on the changes in spatial disposition of the spectator ligands only (method **I**), or on the full associated polyhedron and its infinitely distorted version that results from ligand dissociation (method **II**). In some cases, one can choose to compare the studied structures with the two end points of the association/dissociation reaction, represented by polyhedra with different numbers of vertices (method **III**).

Table 3. Summary of the association pathways studied in this paper.

Coord.[a]	Shapes[b]	Examples	Method	Drawing
4+2	SP-4→*trans*-(OC-6)	Cu^{II}, N^{II}, Mn^{III}, Au^{II} complexes[c] AgF_2, PdS_2, $PdSe_2$	**II**	
	T-4→*cis*-(OC-6)	$NiWO_4$,[c] Ca_2AlFeO_5[c]	**I**, **IV**	Scheme 2
	T-4→*trans*-(OC-6)	TiO_2 (anatase), Ba_2TiO_4, TiO_2 (rutile)	**I**	
2+4	L-2→OC-6	HgO_2, inverted tetragonal Jahn–Teller[c]	**II**	Scheme 3
6+1	OC-6→CO-7	Tripodal ligands **1** and **2**[c]	**III**	
	OC-6→PBPY-7	Ta_2O_5,[c] $KCuAlF_6$,[c] ligand **3**[c]	**I**	Scheme 4
4+3	T-4→CO-7	$Mg(AlH_4)_2$, $A_2M_3O_8$ (hollandite)[c]	**I**	Scheme 5
4+4	T-4→DD-8	$La_2(WO_4)_3$,[c] UCl_4[c]	**I**	Scheme 6 D_{2d}
	T-4→GBF-8	$[Cd(NO_3)_4]^{2-}$	**I**	Scheme 6 D_2
	SP-4→CU-8	"Pd_{13}"	**I**	Scheme 6 D_{2h}
6+2	OC-6→HBPY-8	PdF_2[c]	**I**, **IV**	Scheme 7
	OC-6→CU-8	$NiWO_4$,[c] $YbTaO_4$[c]	**I**	Scheme 8

[a] An *n*+*m* coordination stands for *n* metal–ligand bonds and *m* secondary interactions. [b] Abbreviations: L-2, linear; T-4, tetrahedron; SP-4, regular square; OC-6, octahedron; CO-7, capped octahedron; PBPY-7, pentagonal bipyramid; DD-8, triangular dodecahedron; GBF-8, gyrobifastigium; HBPY-8, hexagonal bipyramid; CU-8, cube. [c] Refers to several compounds with the indicated structural type.

The continuous shape measures methodology has been applied, inter alia, to Jahn–Teller active metal ions such as Cu^{II}, Au^{II}, and Mn^{III}. The results show how arbitrary it may be in many instances to distinguish between four- and six-coordinated Cu^{II} complexes. A related topic that has been discussed is the possibility of distinguishing in a systematic way amenable to automatization between elongation tetragonal Jahn–Teller distortions and the less common tetragonal compression distortion. A study of Ni^{II} compounds shows how the coordinative unsaturation of this metal ion results in a continuity of geometries from strictly square planar to perfectly octahedral, with structures covering the whole range of intermediate situations with four strongly bound ligands and two more or less weakly coordinated Lewis bases.

In our analysis, we have considered not only structural correlations, but also temperature- and pressure-dependent structural changes, as well as spin-crossover behavior associated with polyhedral rearrangements.

Computational Methods

For the calculation of the shape measures reported in this paper, we have used the SHAPE program,[73] which can be obtained from the authors upon request. The structural data analyzed was retrieved from the Cambridge Structural Database,[74] version 5.30, and from the ICSD.[75]

Acknowledgements

This work has been supported by the Ministerio de Invesigación, Ciencia e Innovación (MICINN), project CTQ2008-06670-C02-01-BQU, and by Generalitat de Catalunya, grants 2009SGR-1459 and XRQTC.

[1] S. Alvarez, P. Alemany, D. Casanova, J. Cirera, M. Llunell, D. Avnir, *Coord. Chem. Rev.* **2005**, *249*, 1693.
[2] D. Casanova, J. Cirera, M. Llunell, P. Alemany, D. Avnir, S. Alvarez, *J. Am. Chem. Soc.* **2004**, *126*, 1755.
[3] L. Pauling, *The Nature of the Chemical Bond*, 3rd ed., Cornell University Press, Ithaca, **1960**.
[4] R. H. Kretsinger, F. A. Cotton, R. F. Bryan, *Acta Crystallogr.* **1963**, *16*, 651.
[5] W. Levason, R. Ratnani, G. Reid, M. Webster, *Inorg. Chim. Acta* **2006**, *359*, 4627; M. D. Brown, W. Levason, D. C. Murray, M. C. Popham, G. Reid, M. Webster, *Dalton Trans.* **2003**, 857; G. Ferguson, K. E. Matthes, D. Parker, *Angew. Chem.* **1987**, *99*, 1195; *Angew. Chem. Int. Ed. Engl.* **1987**, *26*, 1162.
[6] R. L. Lucas, M. K. Zart, J. Murkerjee, T. N. Sorrell, D. R. Powell, A. S. Borovik, *J. Am. Chem. Soc.* **2006**, *128*, 15476.
[7] B. M. Fung, *J. Am. Chem. Soc.* **1967**, *89*, 5788.
[8] O. Jeannin, R. Clérac, T. Cauchy, M. Fourmigué, *Inorg. Chem.* **2008**, *47*, 10656.
[9] G. Marangoni, B. Pitteri, V. Bertolasi, V. Ferretti, G. Gilli, *J. Chem. Soc. Dalton Trans.* **1987**, 2235.
[10] S. Groysman, R. H. Holm, *Inorg. Chem.* **2009**, *48*, 621.
[11] J. A. Krause Bauer, S. E. Edison, M. J. Baldwin, *Acta Crystallogr. Sect. E* **2005**, *61*, m82.
[12] T. Nguyen, A. Panda, M. M. Olmstead, A. F. Richards, M. Stender, M. Brynda, P. P. Power, *J. Am. Chem. Soc.* **2005**, *127*, 8545.
[13] P. P. Power, *Comments Inorg. Chem.* **1989**, *8*, 177; P. P. Power, *J. Organomet. Chem.* **2004**, *689*, 3904.
[14] W. Baratta, S. Stoccoro, A. Doppiu, E. Herdtweck, A. Zucca, P. Rigo, *Angew. Chem.* **2003**, *115*, 109; *Angew. Chem. Int. Ed.* **2003**, *42*, 105.
[15] W. Baratta, E. Herdtweck, *Angew. Chem.* **1999**, *111*, 1733; *Angew. Chem. Int. Ed.* **1999**, *38*, 1629; N. M. Scott, V. Pons, E. D. Stevens, D. M. Heinekey, S. P. Nolan, *Angew. Chem.* **2005**, *117*, 2568; *Angew. Chem. Int. Ed.* **2005**, *44*, 2512.
[16] H.-B. Bürgi, V. Shklover in *Perspectives in Coordination Chemistry* (Eds.: A. F. Williams, C. Floriani, A. E. Meerbach), Helvetica Chimica Acta, Basel, **1992**.
[17] M. A. Carvajal, S. Alvarez, J. J. Novoa, *J. Am. Chem. Soc.* **2004**, *126*, 1465; X.-Y. Liu, F. Mota, P. Alemany, J. J. Novoa, S. Alvarez, *Chem. Commun.* **1998**, 1149.
[18] A. G. Blackman, *C. R. Chim.* **2005**, *8*, 107.
[19] P. Guionneau, F. Le Gac, A. Kaiba, J. Sánchez Costa, D. Chasseau, J.-F. Létard, *Chem. Commun.* **2007**, 3723.
[20] P. Guionneau, J. Sánchez Costa, J.-F. Létard, *Acta Crystallogr. Sect. C* **2004**, *60*, m587.
[21] F. Schossberger, *Z. Krist. Kristallgeom. Kristallphys. Kristallchem.* **1942**, *104*, 358.
[22] J. R. Guenter, G. B. Jameson, *Phase Transitions* **1992**, *38*, 127; K. K. Wu, I. D. Brown, *Acta Crystallogr. Sect. A* **1973**, *29*, 2009.
[23] J. Kissel, R. Hoppe, *Z. Anorg. Allg. Chem.* **1990**, *582*, 103.
[24] D. Casanova, P. Alemany, S. Alvarez, *Angew. Chem.* **2006**, *118*, 1485; *Angew. Chem. Int. Ed.* **2006**, *45*, 1457.
[25] S. Alvarez, D. Avnir, M. Llunell, M. Pinsky, *New J. Chem.* **2002**, *26*, 996.
[26] M. Pinsky, D. Avnir, *Inorg. Chem.* **1998**, *37*, 5575.
[27] J. Cirera, E. Ruiz, S. Alvarez, *Chem. Eur. J.* **2006**, *12*, 3162.
[28] M. Pinsky, D. Casanova, P. Alemany, S. Alvarez, D. Avnir, C. Dryzun, Z. Kizner, A. Sterkin, *J. Comput. Chem.* **2008**, *29*, 190.
[29] S. Alvarez, M. Llunell, *J. Chem. Soc. Dalton Trans.* **2000**, 3288.
[30] P. B. Durand, E. M. Holt, *Acta Crystallogr. Sect. A* **1995**, *51*, 850.
[31] O. J. Parker, G. L. Breneman, *Acta Crystallogr. Sect. A* **1995**, *51*, 1097.
[32] B. Cordero, V. Gómez, A. E. Platero-Prats, M. Revés, J. Echeverría, E. Cremades, F. Barragán, S. Alvarez, *Dalton Trans.* **2008**, 2832.
[33] J.-P. Wang, W. Wang, J.-Y. Niu, *Jiegou Huaxue* **2007**, *26*, 194.

[34] J. C. Tedenac, N. D. Phung, C. Avinens, M. Maurin, *J. Inorg. Nucl. Chem.* **1976**, *38*, 85.
[35] A. Skorupa, B. Korybut-Daszkiewicz, J. Mrozinski, *Inorg. Chim. Acta* **2002**, *336*, 65.
[36] P. H. Davis, L. K. White, R. L. Belford, *Inorg. Chem.* **1975**, *14*, 1753.
[37] C. P. Kulatilleke, S. N. Goldie, M. J. Heeg, L. A. Ochrymowycz, D. B. Rorabacher, *Inorg. Chem.* **2000**, *39*, 1444.
[38] M. Ciampolini, N. Nardi, P. Dapporto, P. Innocenti, F. Zanobini, *J. Chem. Soc. Dalton Trans.* **1984**, 575.
[39] K. T. Szacilowski, P. Xie, A. Y. S. Malkhasian, M. J. Heeg, M. Y. Udugala-Ganehenege, L. E. Wenger, J. F. Endicott, *Inorg. Chem.* **2005**, *44*, 6019.
[40] G. J. Redhammer, G. Tippelt, G. Roth, G. Amthauer, *Am. Mineral.* **2004**, *89*, 405.
[41] C. B. Vanpeteghem, R. J. Angel, J. Zhao, N. L. Ross, G. J. Redhammer, F. Seifert, *Phys. Chem. Miner.* **2008**, *35*, 493.
[42] G. Roth, P. Adelmann, R. Knkitter, S. Massing, T. Wolf, *J. Solid State Chem.* **1992**, *99*, 376.
[43] C. de La Calle, J. A. Alonso, A. Aguadero, M. T. Fernández, *Dalton Trans.* **2009**, 4104.
[44] J. Forniés, B. Menjón, R. M. Sanz-Carrillo, M. Tomás, N. G. Connelly, J. G. Crossley, G. A. Orpen, *J. Am. Chem. Soc.* **1995**, *117*, 4295; M. P. García, M. V. Jiménez, A. Cuesta, C. Siurana, L. A. Oro, F. J. Lahoz, J. A. López, M. P. Catalán, A. Tiripicchio, M. Lanfranchi, *Organometallics* **1997**, *16*, 1026.
[45] F. A. Jalón, B. R. Manzano, M. L. Soriano, I. M. Ortiz in *Supramolecular Catalysis, Vol. 3* (Ed.: P. W. N. M. van Leeuwen), Wiley-VCH, Weinheim, **2008**, p. 57.
[46] For a recent analysis of the structures of Group 14 elements, see: X.-D. Wen, T. Cahill, R. Hoffmann, *Chem. Eur. J.* **2010**, *16*, DOI: 10.1002/chem.200903128.
[47] V. T. Deshpande, D. B. Sirdeshmukh, *Acta Crystallogr.* **1962**, *15*, 294; M. I. McMahon, R. J. Nelmes, N. G. Wright, D. R. Allan, *Z. Kristallogr.* **2004**, *219*, 376; S. B. Qadri, E. F. Skelton, A. W. Webb, *Science* **1963**, *139*; D. R. Allan, R. J. Nelmes, M. I. McMahon, S. A. Belmonte, T. Bovornratanaraks, *Rev. High Pressure Sci. Technol.* **1998**, *7*, 236; U. Schwarz, *Z. Kristallogr.* **2004**, *219*, 376.
[48] N. G. Vannerberg, *Ark. Kemi* **1959**, *13*, 515.
[49] M. Tsunoda, F. P. Gabbai, *J. Am. Chem. Soc.* **2000**, *122*, 8335.
[50] M. A. Halcrow, *Dalton Trans.* **2003**, 4375.
[51] L. R. Falvello, *Dalton Trans.* **1997**, 4463.
[52] J. M. Holland, X. Liu, J. P. Zhao, F. E. Mabbs, C. A. Kilner, M. Thornton-Pett, M. A. Halcrow, *J. Chem. Soc. Dalton Trans.* **2000**, 3316.
[53] N. K. Solanki, M. A. Leech, E. J. L. McInnes, J. P. Zhao, F. E. Mabbs, N. Feeder, J. A. K. Howard, J. E. Davies, J. M. Rawson, M. A. Halcrow, *J. Chem. Soc. Dalton Trans.* **2001**, 2083; N. K. Solanki, E. J. L. McInnes, F. E. Mabbs, S. Radojevic, M. McPartlin, N. Feeder, J. E. Davies, M. A. Halcrow, *Angew. Chem.* **1998**, *110*, 2344; *Angew. Chem. Int. Ed.* **1998**, *37*, 2221.
[54] D. Casanova, J. M. Bofill, P. Alemany, S. Alvarez, *Chem. Eur. J.* **2003**, *9*, 1281.
[55] I. Morgenstern-Badarau, F. Lambert, J.-P. Renault, M. Cesario, J.-D. Marechal, F. Maseras, *Inorg. Chim. Acta* **2000**, *297*, 338.
[56] A. Deroche, I. Morgenstern-Badarau, M. Cesario, J. Guilhem, B. Keita, L. Nadjo, C. Houee-Levin, *J. Am. Chem. Soc.* **1996**, *118*, 4567; M. Qian, S.-H. Gou, L. He, Y.-M. Zhou, C.-Y. Duan, *Acta Crystallogr. Sect. A* **1999**, *55*, 742.
[57] Y. Sunatsuki, M. Sakata, S. Matsuzaki, N. Matsumoto, M. Kojima, *Chem. Lett.* **2001**, 1254.
[58] M. A. Hoselton, L. J. Wilson, R. S. Drago, *J. Am. Chem. Soc.* **1975**, *97*, 1722.
[59] M. Seredyuk, A. B. Gaspar, J. Kusz, G. Bednarek, P. Gütlich, *J. Appl. Crystallogr.* **2007**, *40*, 1135.
[60] F. Bonadio, M.-C. Senna, J. Ensling, A. Sieber, A. Neels, H. Stoeckli-Evans, S. Decurtins, *Inorg. Chem.* **2005**, *44*, 969; M. G. B. Drew, A. H. B. Othman, S. G. McFall, P. D. A. McIlroy, S. M. Nelson, *J. Chem. Soc. Dalton Trans.* **1977**, 1173; C. Paraschiv, M. Andruh, Y. Journaux, Z. Zak, N. Kyritsakas, L. Ricard, *J. Mater. Chem.* **2006**, *16*, 2660; J. Wang, B. Slater, A. Alberola, H. Stoeckli-Evans, F. S. Razavi, M. Pilkington, *Inorg. Chem.* **2007**, *46*, 4763; S. Hayami, Z.-Z. Gu, Y. Einaga, Y. Kobayashi, Y. Ishikawa, Y. Yamada, A. Fujishima, O. Sato, *Inorg. Chem.* **2001**, *40*, 3240.
[61] M. Müller, B. G. Mueller, *Z. Anorg. Allg. Chem.* **1995**, *621*, 1385; B. G. Müller, *J. Fluorine Chem.* **1981**, *17*, 317; N. Ruchaud, J. Grannec, A. Tressaud, P. Gravereau, *Compt. Rend. Ser. II* **1995**, *321*, 507; Z. Mazej, I. Arcon, P. Benkic, A. Kodre, A. Tressaud, *Chem. Eur. J.* **2004**, *10*, 5052.
[62] A. Fossdal, H. W. Brinks, M. Fichtner, B. C. Hauback, *J. Alloys Compd.* **2005**, *387*, 47.
[63] P. Vajeeston, P. Ravindran, A. Kjekshus, H. Fjellvag, *Appl. Phys. Lett.* **2006**, *89*, 071906.
[64] S. Allen, R. J. Ward, M. R. Hampson, R. K. B. Gover, J. S. O. Evans, *Acta Crystallogr. Sect. B* **2004**, *60*, 32.
[65] R. Shen, C. Wang, T. Wang, C. Dong, X. Chen, J. Liang, *Rare Met.* **2003**, *22*, 49.
[66] D. Casanova, M. Llunell, P. Alemany, S. Alvarez, *Chem. Eur. J.* **2005**, *11*, 1479.
[67] U. Rajalingam, P. A. W. Dean, H. A. Jenkins, M. Jennings, J. M. Hook, *Can. J. Chem.* **2001**, *79*, 1330.
[68] S. Alvarez, *Dalton Trans.* **2005**, 2209.
[69] E. V. Chubarova, M. H. Dickman, B. Keita, L. Nadjo, F. Miserque, M. Mifsud, I. W. C. E. Arends, U. Kortz, *Angew. Chem.* **2008**, *120*, 9685; *Angew. Chem. Int. Ed.* **2008**, *47*, 9542.
[70] J. Haines, J. M. Léger, F. Gorelli, D. D. Klug, J. S. Tse, Z. Q. Li, *Phys. Rev. B* **2001**, *64*, 134110.
[71] Z. Mazej, A. Tressaud, J. Darriet, *J. Fluorine Chem.* **2001**, *110*, 139.
[72] J. A. Thompson, M. E. Barr, D. K. Ford, L. A. Silks III, J. McCormick, P. H. Smith, *Inorg. Chem.* **1996**, *35*, 2025; R. E. Marsh, *Acta Crystallogr. Sect. A* **2004**, *60*, 252; J. Coyle, M. G. B. Drew, C. J. Harding, J. Nelson, R. M. Town, *J. Chem. Soc. Dalton Trans.* **1997**, 1123; H. Chen, X.-Y. Xu, J. Gao, X.-J. Yang, L.-D. Lu, X. Wang, *Jiegou Huaxue* **2005**, *24*, 1276; D. C. Apperley, W. Clegg, S. Cloles, J. L. Coyle, N. Martin, B. Maubert, V. McKee, J. Nelson, *J. Chem. Soc. Dalton Trans.* **1999**, 229.
[73] M. Llunell, D. Casanova, J. Cirera, J. M. Bofill, P. Alemany, S. Alvarez, M. Pinsky, D. Avnir, SHAPE, version 1.21, Barcelona, **2003**.
[74] F. H. Allen, *Acta Crystallogr. Sect. A* **2002**, *58*, 380; I. J. Bruno, J. C. Cole, P. R. Edgington, M. Kessler, C. F. Macrae, P. McCabe, J. Pearson, R. Taylor, *Acta Crystallogr. Sect. B* **2002**, *58*, 389.
[75] A. Belsky, M. Hellenbrandt, V. L. Karen, P. Lucksch, *Acta Crystallogr. Sect. A* **2002**, *58*, 364.

Received: October 29, 2009
Published online: April 22, 2010

